Spectrochimica Acta Part A: Molecular and Biomolecular Spectroscopy 149 (2015) 516–522

Contents lists available at ScienceDirect

Spectrochimica Acta Part A: Molecular and Biomolecular Spectroscopy

journal homepage: www.elsevier.com/locate/saa

Rapid discrimination of three marine fish surimi by Tri-step infrared spectroscopy combined with Principle Component Regression

Yuan Liu [a], Wei Hu [a], Xiao-Xi Guo [a], Xi-Chang Wang [a], Su-Qin Sun [b], Chang-Hua Xu [a,*]

[a] College of Food Science & Technology, Shanghai Ocean University, Shanghai 201306, PR China
[b] Analysis Center, Tsinghua University, Beijing 100084, PR China

HIGHLIGHTS

- The chemical composition of three marine fish surimi were analyzed by IR spectroscopy comprehensively.
- Tri-step infrared spectroscopy combined with PCR was developed to discriminate three marine fish surimi.
- Sixty different surimi samples (twenty for each surimi) were objectively classified by PCR.

GRAPHICAL ABSTRACT

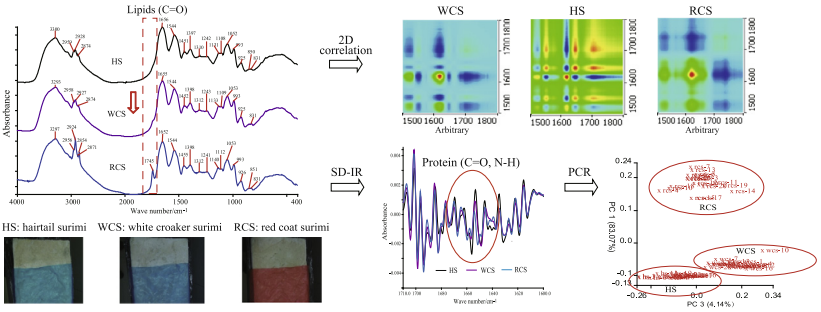

ARTICLE INFO

Article history:
Received 27 January 2015
Accepted 30 April 2015
Available online 7 May 2015

Keywords:
Marine fish surimi
IR macro-fingerprint
Discrimination
PCR

ABSTRACT

A Tri-step infrared spectroscopy (Fourier transform infrared spectroscopy (FT-IR) integrated with second derivative infrared (SD-IR) spectroscopy and two-dimensional correlation infrared spectroscopy (2DCOS-IR)) combined with Principal Component Regression (PCR) were employed to characterize and discriminate three marine fish surimi (white croaker surimi (WCS), hairtail surimi (HS) and red coat surimi (RCS)). The three surimi had similar IR macro-fingerprints (similarity > 0.7) especially for the absorption bands of amide groups. Compared to the other two surimi, however, RCS had a middle strong characteristic peak of lipids at 1745 cm^{-1}, indicating that RCS had the highest content of lipids. SD-IR spectra of the three surimi enhanced the spectral resolution and amplified the small differences, especially at about 1682 cm^{-1}, 1679 cm^{-1}, 1656 cm^{-1} and 1631 cm^{-1}, suggesting that the three had different profiles of proteins. Moreover, evident differences were observed in 2DCOS-IR spectra of 1500–1800 cm^{-1}. WCS had one strong (1620 cm^{-1}) and three weak auto-peaks (1520 cm^{-1}, 1552 cm^{-1}, 1706 cm^{-1}). HS had three strong (1621 cm^{-1}, 1648 cm^{-1}, 1708 cm^{-1}) and two weak auto-peaks (1523 cm^{-1}, 1553 cm^{-1}), whereas RCS had one strong (1623 cm^{-1}) and three weak auto-peaks (1525 cm^{-1}, 1709 cm^{-1}, 1738 cm^{-1}). Furthermore, sixty batches of surimi (twenty for each surimi) were objectively classified by PCR. It was demonstrated that the Tri-step infrared spectroscopy combined with PCR could be applicable for discrimination of precious marine fish surimi in a direct, rapid and holistic manner.

Introduction

"Surimi" is defined as a refined fish protein product prepared mechanically by deboning, mincing and washing processes to remove blood, lipids, enzymes and sarcoplasmic proteins, dehydrated and then stabilized with cryoprotectants before

* Corresponding author.
E-mail address: chxu@shou.edu.cn (C.-H. Xu).

http://dx.doi.org/10.1016/j.saa.2015.04.116
1386-1425/

ice-storage [1]. As a high-protein, low-fat and ready-to-cook fish product, surimi is gaining more prominence worldwide. As surimi loses the original appearance of the corresponding fish and feasible industry standards and national standards to assess the merits and adulteration of surimi are still lacking, driven by high economic interests, surimi adulteration has been frequently occurring [2].

Surimi species identification is mainly based on fish species discrimination. Structural proteins can reflect the genetic characteristics differences of surimi species, so that fish protein electrophoresis analysis techniques, fish protein immunoassay techniques, DNA fingerprinting analysis techniques are generally used to identify fish species [3,4]. However, most of these methods are either time consuming, destructive or require well-trained personnel, and are therefore not applicable for non-destructive and rapid testing in contrast to spectroscopic techniques.

Fourier transform infrared spectroscopy (FT-IR) is a rapid, non-destructive and easy to handle molecular spectroscopic method with high signal-to-noise ratio and good repeatability to analyze complicated mixture systems such as food, Chinese herbal medicine [5–7]. Second derivative infrared spectroscopy (SD-IR) can be used to handle severely overlapped spectra and enhance the apparent resolution. If the differences in FT-IR and SD-IR spectra are too small to tell, two-dimensional correlation infrared spectroscopy (2DCOS-IR) can be employed to unfold FT-IR spectra in a second dimension to identify the differences more remarkably and convincingly [8]. With the holistic analytical method, "Tri-step infrared spectroscopy" (FT-IR combined with SD-IR and 2DCOS-IR), extensive and exact analysis and identification of complicated mixture systems can be achieved [9]. Cluster analysis is the task of grouping a set of objects in such a way that objects in the same group (called a cluster) are more similar (in some sense or another) to each other than to those in other groups (clusters). It is a main task of exploratory data mining, and a common technique for statistical data analysis used in many fields, including machine learning, pattern recognition, image analysis, information retrieval, and bioinformatics [10–12]. Among the methods of cluster analysis, Principle Component Regression (PCR) is a reliable statistical method for classification/discrimination of massive samples. As surimi is a multi-component mixture, application of spectral classification can better reflect the integrity of the sample.

In this study, we attempt to establish a method, Tri-step infrared spectroscopy combined with PCR, to comprehensively analyze and appraise three species of marine fish surimi, white croaker (*Argyrosomus argentatus*) surimi (WCS), hairtail (*Trichiurus haumela*) surimi (HS) and red coat (*Nemipterus virgatus*) surimi (RCS) in a quick, effective and holistic manner.

Experimental

Apparatus

Thermo Scientific Nicolet iS5 spectrometer, equipped with a DTGS detector, in the range of 4000–400 cm^{-1} with a resolution of 4 cm^{-1}. Spectra were recorded with 16 scans. The interferences of H_2O and CO_2 were subtracted when scanning. The heated plate for the multiple reflection Horizontal ATR units (HATRPlus) contains two cartridge heaters used to heat the crystal plate and ensure even heating of the crystal and the sample. The temperature of the block is monitored and controlled by a Resistive Thermal Detector (RTD).

Kjeltec 8400 Analyzer Unit (Foss, Sweden); Soxtec2050 (FOSS, Denmark); Blast Oven DHG-9140A (Shanghai HuiTai Instrument Manufacturing Co., China); Muffle furnace SXL-1002 (Shanghai Jing Hong Experimental Equipment Co., China); Freeze Dryer BTP-3XLOVX (Virtis, American).

Materials

Three frozen AAA grade marine fish surimi (white croaker (*Argyrosomus argentatus*) surimi (WCS), hairtail (*Trichiurus haumela*) surimi (HS) and red coat (*Nemipterus virgatus*) surimi (RCS)) were collected from Shanghai Caixing Food Company.

Procedure

Chemical composition analysis

Moisture content was determined using method namely oven-dry (AOAC 950.46, 2007). The fat content of the sample was determined as free fat, and extracted from sample by Soxhlet (AOAC 960.39, 2007) using ether as solvent. Protein content was estimated from nitrogen ($N \times 6.25$) using constant Kjeldahl method (AOAC 981.10, 2007). The ash content of the sample was determined using methods called Muffle furnace ashing (AOAC, 938.08, 2007). TVB-N content was estimated as follows: 5.0 g of each sample (WCS, HS and RCS) was placed in digestive tract, adding 0.5 g Magnesia, and determined by automatic Kjeldahl analyzer (see Fig. 1).

IR acquisition

WCS, HS and RCS was thawed overnight at 4 °C [13]. Then the surimi was freeze-dried for 24 h and pulverized into fine powder; 1–2 mg of each sample was blended with KBr powder, ground again, and pressed into a tablet. The FT-IR spectra of all samples were collected at room temperature. The raw FT-IR data was processed with Omnic spectrum software (Version 9.2.106) of Thermo FT-IR spectrometer. All the second derivative IR spectra were obtained after 13-point smoothing of the original IR spectra.

2DCOS-IR acquisition

The thawed surimi samples were placed in ATR accessory, connected with the temperature controller. The temperature range was from 30 °C to 70 °C and the dynamic original spectra at different temperatures were collected at an interval of 5 °C. 2DCOS-IR spectra were obtained by analyzing the series of temperature-dependent dynamic spectra with 2DCOS-IR correlation analysis software designed by Thermo (Nicolet iN10 SpectraCorr).

Cluster analysis

60 samples (20 for each surimi) were also freeze-dried for 24 h and pulverized into fine powder; 1–2 mg of each sample was blended with KBr powder, ground again, and pressed into a tablet. Cluster analysis was carried out by using PCR (PerkinElmer, UK) and the region was conducted in the range of 1800–800 cm^{-1}.

Results and discussion

Chemical analysis of three surimi

The contents of proteins, lipids, moisture, ash and TVB-N have analyzed and the results are summarized in Table 1.

IR spectra of three surimi

Surimi mainly consists of proteins in dry weight (Table 1). Generally, the peaks in amide I absorption bands (~1655 cm^{-1}) and amide II absorption bands (~1544 cm^{-1}) are prevalently

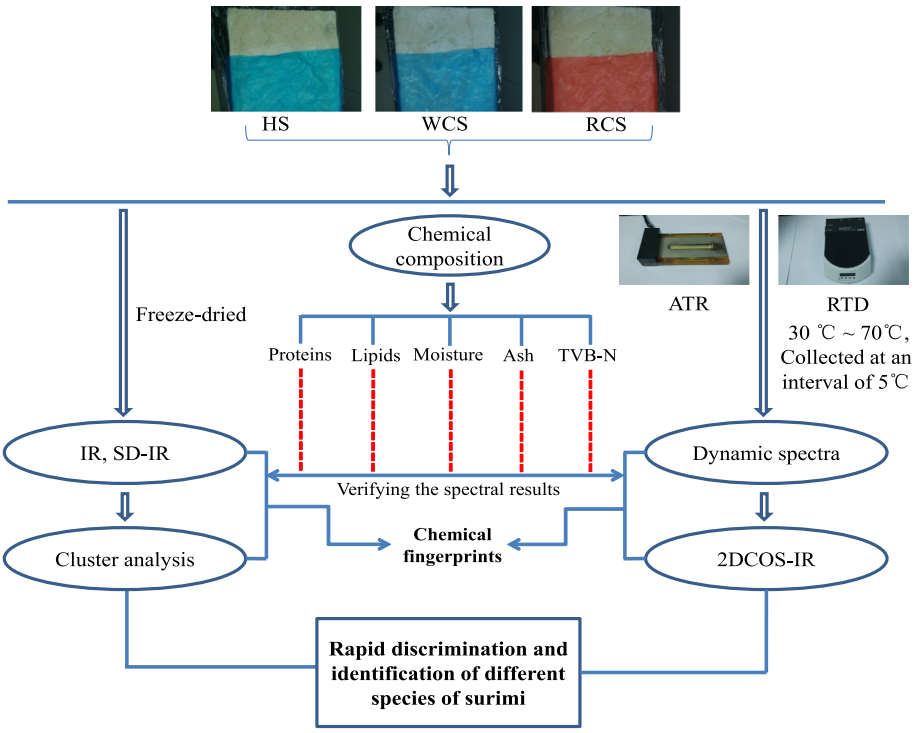

Fig. 1. The scheme of experimental design.

Table 1
Chemical composition of three species of surimi.

Chemical composition	HS	WCS	RCS
Proteins (%)	19.83 ± 0.16[a]	15.71 ± 0.13[b]	14.84 ± 0.13[c]
Lipids (%)	**0.18 ± 0.02[b]**	**0.25 ± 0.05[b]**	**0.47 ± 0.02[a]**
Moisture (%)	71.97 ± 0.12[c]	75.59 ± 0.08[a]	74.99 ± 0.12[b]
Ash (%)	0.68 ± 0.04[a]	0.53 ± 0.007[a]	0.61 ± 0.14[a]
TVB-N (mg/100 g)	4.57 ± 0.12[a]	3.32 ± 0.18[c]	3.96 ± 0.26[c]

Note: Values in the table denote the mean ± standard error; different superscript letters in the same line represent significant difference; Figures in bold indicate a significant increasing trend of lipids for the three surimi from HS to RCS.

strong and subsequently the spectra of three species of surimi are similar (spectral correlation coefficient > 0.7) (Fig. 2), despiting that the position, intensity, and shape of some peaks in the conventional IR spectra are different. Compared to the other two surimi, however, RCS has a middle strong characteristic peak of lipids at 1745 cm^{-1}, indicating that the lipids content in RCS is higher than those in the other two surimi. This finding was confirmed by our chemical composition studies (Table 1). In addition, absorption peaks at 1053 cm^{-1}, 993 cm^{-1} and 925 cm^{-1} belonged to white sugar characteristic peaks can be found in the three surimi,

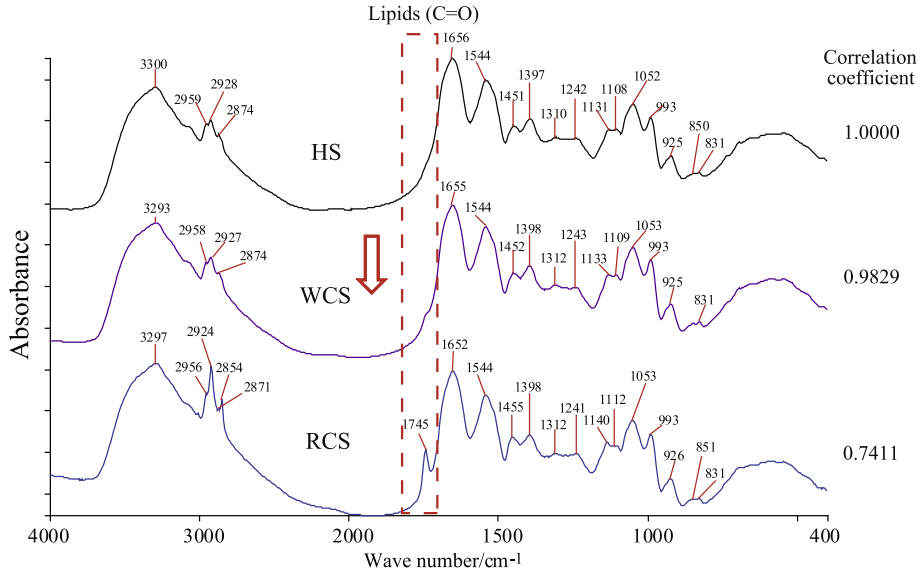

Fig. 2. IR spectra of hairtail surimi (HS), white croaker surimi (WCS) and red coat surimi (RCS). (For interpretation of the references to color in this figure legend, the reader is referred to the web version of this article.)

Table 2
The preliminary assignment of main characteristic absorption peaks of FT-IR spectra of surimi.

Peak position (cm^{-1})	Base group and vibration mode	Main attribution
2930	ν_{as}(C—H)	CH_2
1745	ν_s(C=O)	Carbonyl group
1698–1612	ν(C=O)	Protein
1523–1553	ν(C—N)	Protein
1433	(C—H)	CH_3, CH_2
1053, 993, 925	ν(C—O)	White sugar

Note: ν, stretching mode; δ, bending mode; *s*, symmetric; *as*, asymmetric.

suggesting that white sugar was added in three surimi during processing (see Table 2).

Second derivative IR spectra of three surimi

Generally, second derivative IR spectroscopy can enhance the spectral resolution by amplifying tiny differences in IR spectra. Some overlapped absorption peaks and shoulder peaks can be separated by using second derivative spectral analysis [14]. Fig. 3 shows the second derivative spectra of WCS, HS and RCS. The second derivative IR spectra show differences concerned with peak

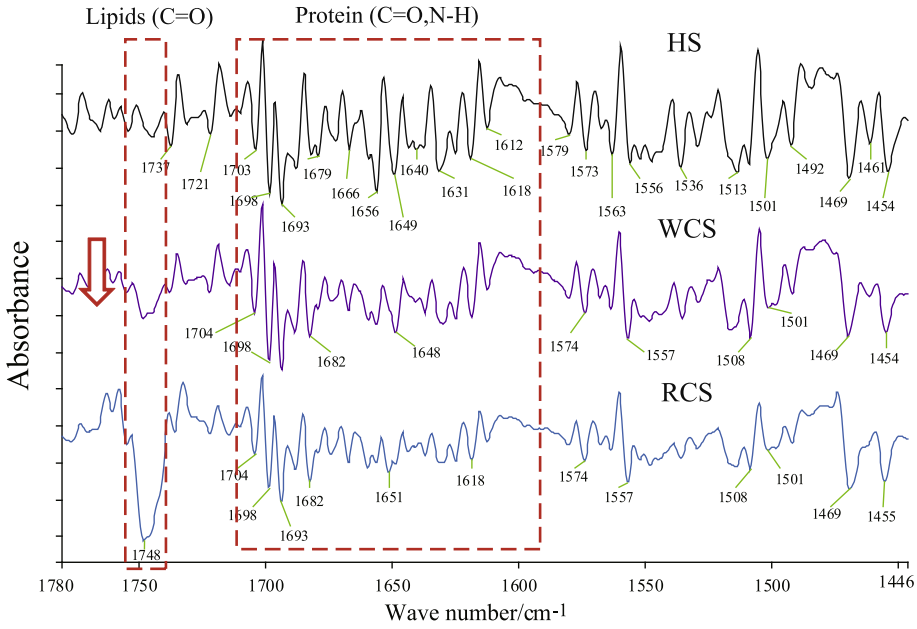

Fig. 3. Second derivative spectra of hairtail surimi (HS), white croaker surimi (WCS) and red coat surimi (RCS) in the region of 1800–1400 cm^{-1}. (For interpretation of the references to color in this figure legend, the reader is referred to the web version of this article.)

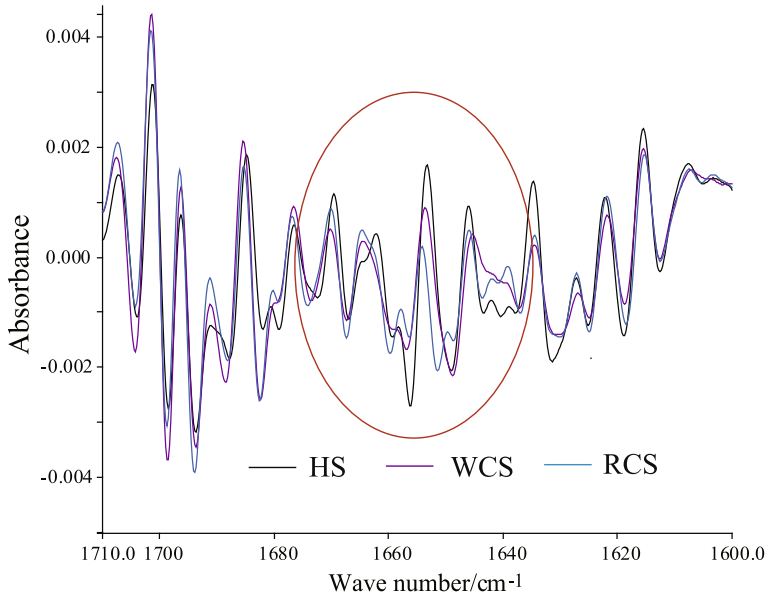

Fig. 4. Second derivative spectra of hairtail surimi (HS), white croaker surimi (WCS) and red coat surimi (RCS) in the region of 1710–1600 cm^{-1}. (For interpretation of the references to color in this figure legend, the reader is referred to the web version of this article.)

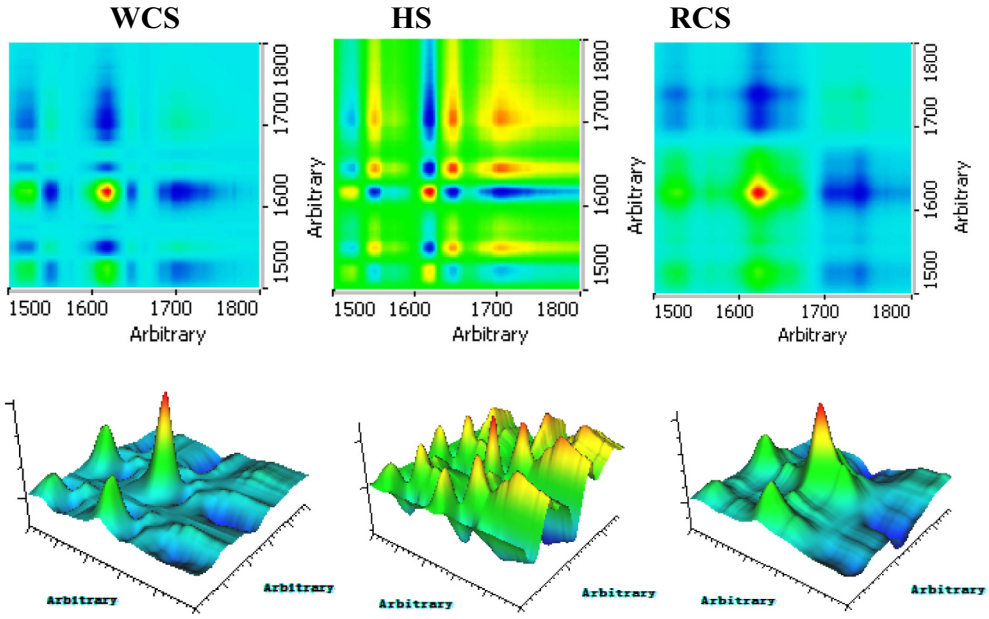

Fig. 5. 2DCOS-IR synchronous spectra of white croaker surimi (WCS), hairtail surimi (HS) and red coat surimi (RCS) in the region of 1800–1500 cm^{-1}. (For interpretation of the references to color in this figure legend, the reader is referred to the web version of this article.)

Table 3
Auto-peaks in 2DCOS-IR synchronous spectra of WCS, HS and RCS.

Surimi	Autopeaks (cm^{-1})				
White croaker	1520	1552	**1620**	1706	
Hairtail	1523	1553	**1621**	**1648**	**1708**
Red coat	1525	**1623**	1709	1738	

Notes: Peaks in bold are the strong auto-peaks; peaks in underline are in negative correlation with other auto-peaks.

Table 4
Parameters for model based on PCR.

Parameters	Values
Analysis range	1800–800 cm^{-1}
Scaling (spectra)	Mean
Smooth	–
Baseline correction	First derivative, 5 point
Normalization	SNV de-trending

position particularly in the range of 1800–1400 cm^{-1}, and especially the differences on lipids content of three surimi become more apparent. In 1710–1600 cm^{-1} of amide I absorption band, different peak positions, shapes and intensities indicate that the three have different profiles of proteins (Fig. 4). Compared to the other two surimi, HS has strong absorption peaks at 1679 cm^{-1}, 1656 cm^{-1} and 1631 cm^{-1}, while the peak at 1682 cm^{-1} in WCS and RCS is much stronger. Moreover, HS has the strongest absorption peaks at 1461 cm^{-1}, 1433 cm^{-1} and 1422 cm^{-1}, sequentially followed by WCS and RCS. Thus, these three species of surimi can be further differentiated by their second derivative IR spectra.

2DCOS-IR spectra of three surimi

In order to identify differences among the three surimi more convincingly, 2DCOS-IR has been employed in the range of 1800–1500 cm^{-1}. 2DCOS-IR spectroscopy can improve the resolution of spectrum and provide more information by showing the influences of the perturbation on each of molecules in the sample and then processing the data by a mathematical correlation analysis technique [15–18]. The 2DCOS-IR correlation spectra illustrate the sensitivity for each IR band or functional group and correlation between the functional groups, as well as the sequence of responses, when the investigated system is subjected to a given perturbation. The peaks (auto-peaks and cross-peaks) in the synchronous 2D correlation spectrum represent the coincidence of the spectral intensity variations at corresponding variables along the perturbation and can be used to authenticate differences between samples. In 2DCOS-IR spectra, positive correlation

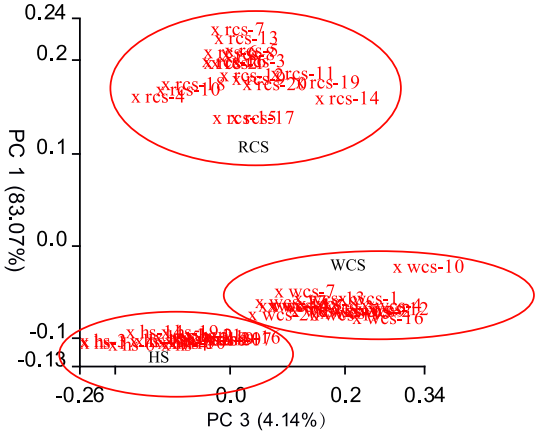

Fig. 6. Classification plot of PCR analysis for FT-IR data of 20 WCS, 20 HS and 20 RCS.

(red/green area) indicates that a group of absorption bands change simultaneously (either stronger or weaker), while negative correlation (blue area) is just the reverse [19].

The differences among three surimi can be described further through the synchronous 2DCOS-IR spectra. Fig. 5 are the synchronous 2DCOS-IR spectra of three surimi in the range of 1800–1500 cm^{-1}. For easy comparison, the information (peak positions, relative intensities) and correlationship of auto-peaks are summarized in Table 3. During the temperature increasing from 30 °C to 70 °C, WCS has one strong auto-peak at 1620 cm^{-1} and three weak

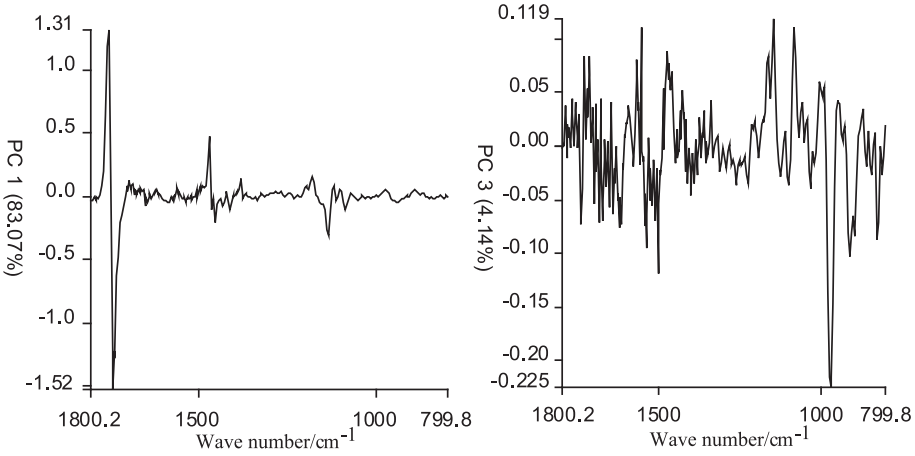

Fig. 7. Plot of PC1 (left) and PC3 scores (right).

auto-peaks at 1520 cm^{-1}, 1552 cm^{-1} and 1706 cm^{-1}. HS has three strong auto-peaks at 1621 cm^{-1}, 1648 cm^{-1} and 1708 cm^{-1} and two weak auto-peaks at 1523 cm^{-1} and 1553 cm^{-1}, whereas RCS has one strong auto-peak at 1623 cm^{-1} and three weak auto-peaks 1525 cm^{-1}, 1709 cm^{-1} and 1738 cm^{-1}. Form the all above, heat-sensitivities of the proteins and lipids in three surimi are different, resulting in the evident differences among the 2DCOS-IR spectra. Therefore, the three surimi have respective unique fingerprints in the range of 1800–1500 cm^{-1} which can be used as an exclusive range for the identification of three species of surimi.

Cluster analysis

To establish a convenient classification model for the three surimi, sixty parallel samples (20 WCS, 20 HS and 20 RCS) were investigated and the range of 1800–800 cm^{-1} was selected for principal component regression (PCR). The parameters for establishing surimi classification model are summarized in Table 4.

The three surimi were completely separated (Fig. 6). The dispersion degree of the result reflects component uniformity of the three surimi: RCS samples show obvious variations suggesting that RCS is inhomogeneous, mainly related with the fluctuation of lipids content (Fig. 7). This inhomogeneity impact greatly on surimi quality which is worth of further investigation. Since RCS contains much more lipids than the rest, which leads to completely separation of RCS from the others. The approximate lipids contents of the other two surimi lead to close PC1 scores. The above results demonstrate that WCS, HS and RCS have been classified successfully using IR combined with PCR and the established model could be used to evaluate the unknown surimi samples.

Conclusions

The three different species of surimi, WCS, HS and RCS, have been quickly and effectively distinguished by the Tri-step infrared spectroscopy combined with PCR. In IR spectra, the absorption bands attributed to lipids is the main difference among WCS, HS and RCS. According to fingerprint characters and peak intensity, RCS has relatively higher lipids content comparing to WCS and HS. With applying second derivative infrared spectroscopy, the tiny differences among them have been enlarged. Different peak positions, shapes and intensities in the range of 1710–1500 cm^{-1} indicate that the three have different profiles of proteins, including secondary structure. Finally, through the synchronous 2DCOS-IR spectra in the range of 1800–1500 cm^{-1}, the clear distinctions among the three species have been thoroughly visualized. Moreover, sixty different surimi samples (twenty for each) have been successfully classified by Principal Component Regression (PCR).

It has been demonstrated that the Tri-step infrared spectroscopy combined with cluster analysis could be a scientific and powerful tool for rapid discrimination and identification of different species of surimi in a holistic manner.

Acknowledgement

This work is financially supported by National Natural Science Foundation of China (Grant No. 31401571), Natural Science Foundation of Shanghai (Grant No. 14ZR1420000), and Special Foundation for science and technology development of Shanghai Ocean University (Grant No. A2-0209-14-200059).

References

[1] M. Uddin, E. Okazaki, H. Fukushima, S. Turza, Y. Yumiko, Y. Fukuda, Nondestructive determination of water and protein in surimi by near-infrared spectroscopy, Food Chem. 96 (3) (2006) 491–495.
[2] T. Pepe, M. Trotta, I. Di Marco, A. Anastasio, J.M. Bautista, M.L. Cortesi, Fish species identification in surimi-based products, J. Agric. Food Chem. 55 (9) (2007) 3681–3685.
[3] W. Zhao, Y. Zhao, Y. Pan, X. Wang, Z. Wang, J. Xie, Authentication and traceability of Nibea albiflora from surimi products by species-specific polymerase chain reaction, Food Control 31 (1) (2013) 97–101.
[4] A. Ardura, A.R. Linde, J.C. Moreira, E. Garcia-Vazquez, 2010 DNA barcoding for conservation and management of Amazonian commercial fish, Biol. Conserv. 143 (6) (2010) 1438–1443.
[5] S.-Q. Sun, Q. Zhou, J. Chen, Infrared spectroscopy for complex mixtures: applications in food and traditional Chinese medicine, Chemical Industry Press, 2011.
[6] S.-Q. Sun, Q. Zhou, Z. Qin, Atlas of two-dimensional correlation infrared spectroscopy for traditional Chinese medicine identification, Chemical Industry Press, Beijing, 2003.
[7] C. Xu, Y. Wang, J. Chen, Q. Zhou, P. Wang, Y. Yang, et al., Infrared macro-fingerprint analysis-through-separation for holographic chemical characterization of herbal medicine, J. Pharm. Biomed. Anal. 74 (2013) 298–307.
[8] X.-X. Wu, C.-H. Xu, M. Li, S.-Q. Sun, J.-M. Li, W. Dong, Analysis and identification of two reconstituted tobacco sheets by three-level infrared spectroscopy, J. Mol. Struct. 1069 (2014) 133–139.
[9] J.-R. Li, S.-Q. Sun, X.-X. Wang, C.-H. Xu, J.-B. Chen, Q. Zhou, et al., Differentiation of five species of Danggui raw materials by FTIR combined with 2D-COS IR, J. Mol. Struct. 1069 (2014) 229–235.
[10] W.C. Moore, D.A. Meyers, S.E. Wenzel, W.G. Teague, H. Li, X. Li, et al., Identification of asthma phenotypes using cluster analysis in the severe asthma research program, Am. J. Respir. Crit. Care Med. 181 (4) (2010) 315–323.
[11] M.B. Eisen, P.T. Spellman, P.O. Brown, D. Botstein, Cluster analysis and display of genome-wide expression patterns, Proc. Natl. Acad. Sci. U.S.A. 95 (25) (1998) 14863–14868.

[12] N. Chen, Z.S. Xu, M.M. Xia, Correlation coefficients of hesitant fuzzy sets and their applications to clustering analysis, Appl. Math. Model. 37 (4) (2013) 2197–2211.
[13] X.Y. Wang, X.C. Wang, Y. Liu, R.Y. Dong, Application of near infrared spectroscopy technique based on support vector machine in the measurement of moisture and protein contents in surimi, Spectrosc. Spectr. Anal. 32 (9) (2012) 2418–2421.
[14] S. Sun, J. Chen, Q. Zhou, G. Lu, K. Chan, Application of mid-infrared spectroscopy in the quality control of traditional Chinese medicines, Planta Med. 76 (17) (2010) 1987–1996.
[15] Y. Wang, C.-H. Xu, P. Wang, S.-Q. Sun, J.-B. Chen, J. Li, et al., Analysis and identification of different animal horns by a three-stage infrared spectroscopy, Spectrochim. Acta A 83 (1) (2011) 265–270.
[16] I. Noda, Generalized two-dimensional correlation method applicable to infrared, Raman, and other types of spectroscopy, Appl. Spectrosc. 47 (9) (1993) 1329–1336.
[17] I. Noda, Two-dimensional infrared spectroscopy, J. Am. Chem. Soc. 111 (21) (1989) 8116–8118.
[18] Y.M. Jung, Y. Park, S. Sarker, J.-J. Lee, U. Dembereldorj, S.-W. Joo, Surface-induced thermal decomposition of Ru(dcbpyH)(2)-(CN)(2) on nanocrystalline TiO_2 surfaces: temperature-dependent infrared spectroscopy and two-dimensional correlation analysis, Sol. Energy Mater. Sol. Cells 95 (1) (2011) 326–331.
[19] C. Xu, X. Jia, R. Xu, Y. Wang, Q. Zhou, S. Sun, Rapid discrimination of Herba Cistanches by multi-step infrared macro-fingerprinting combined with soft independent modeling of class analogy (SIMCA), Spectrochim. Acta A Mol. Biomol. Spectrosc. 114 (2013) 421–431.